

Ecosystem photosynthesis inferred from measurements of carbonyl sulphide flux

David Asaf¹, Eyal Rotenberg¹, Fyodor Tatarinov¹, Uri Dicken¹, Stephen A. Montzka² and Dan Yakir^{1*}

Limited understanding of carbon dioxide sinks and sources on land is often linked to the inability to distinguish between the carbon dioxide taken up by photosynthesis, and that released by respiration^{1,2}. Carbonyl sulphide, a sulphur-containing analogue of carbon dioxide, is also taken up by plants, and could potentially serve as a powerful proxy for photosynthetic carbon dioxide uptake, which cannot be directly measured above the leaf scale. Indeed, variations in atmospheric concentrations of carbonyl sulphide are closely related to those of carbon dioxide at regional, local and leaf scales^{3–9}. Here, we use eddy covariance and laser spectroscopy¹⁰ to estimate the net exchange of carbon dioxide and carbonyl sulphide across three pine forests, a cotton field and a wheat field in Israel. We estimate gross primary productivity—a measure of ecosystem photosynthesis—directly from the carbonyl sulphide fluxes, and indirectly from carbon dioxide fluxes. The two estimates agree within an error of ±15%. The ratio of carbonyl sulphide to carbon dioxide flux at the ecosystem scale was consistent with the variability in mixing ratios observed on seasonal timescales in the background atmosphere. We suggest that atmospheric measurements of carbonyl sulphide flux could provide an independent constraint on estimates of gross primary productivity, key to projecting the response of the land biosphere to climate change.

Carbonyl sulphide (COS) is a sulphur-containing analogue of CO₂ with atmospheric mixing ratios of about 500 pmol mol⁻¹ and an atmospheric lifetime of 2–4 years. Its main sources are oxidation of CS₂ and dimethyl sulphide, direct emission from the upper ocean, and anthropogenic sources, and its main sinks are uptake by plants and soils, and oxidation in the stratosphere^{11–13}. COS and CO₂ flux into leaves and soils are influenced by the same physical, diffusion, pathway followed by hydration reactions catalysed by the enzyme carbonic anhydrase. The hydration reaction (equation (1)) is irreversible for COS (ref. 14) making it essentially a one-way flux into the land biosphere:



The possibility that COS flux could be used as a proxy for photosynthetic CO₂ uptake is especially attractive because it is impossible to directly measure this CO₂ flux at scales above the leaf. The simultaneous occurrence of respiration from non-photosynthetic parts of plants and soil microorganisms partially offsets the photosynthetic CO₂ uptake in fields and forests. Ecosystem and local eddy covariance studies can therefore only resolve the net ecosystem CO₂ exchange¹⁵ (NEE).

The COS approach relies on a few key assumptions (co-diffusion but no interactions with CO₂; one-way COS flux; and

negligible competing fluxes to/from soils⁵) that once met allow a direct estimate of net photosynthetic CO₂ assimilation by leaves, and an approximation (see Supplementary Information) of gross primary productivity (GPP) at the flux tower and larger scales according to^{3,5,8}:

$$\frac{\text{GPP}}{[\text{CO}_2]} = \frac{F_{\text{COS}}}{[\text{COS}]} \times \frac{1}{\text{LRU}^*}; \quad \text{GPP} = \frac{F_{\text{COS}}}{\text{LRU}^*} \times \frac{[\text{CO}_2]}{[\text{COS}]} \quad (2)$$

where F_{COS} is the directly measured flux of COS, [COS] and [CO₂] are ambient mixing ratios of COS and CO₂, LRU (estimated at ~1.6; ref. 7) is the leaf-scale normalized ratio of COS to CO₂ assimilation rates, A , ($\text{LRU} = (A_{\text{COS}}/[\text{COS}])/(A_{\text{CO}_2}/[\text{CO}_2])$; refs 3, 6, 8) accounting for differences between COS and CO₂ in diffusivity, dissolution and reaction rates, and the asterisk indicates that A_{CO_2} was adjusted to GPP (accounting for leaf mitochondrial respiration in the light; see Supplementary Information). Ecosystem-scale relative uptake (ERU; recently estimated to be ~4; ref. 5), which is not required for estimating GPP on the basis of equation (2), provides, nevertheless, a link to atmospheric measurements and can be defined on the basis of net ecosystem exchange of COS (F_{COS}) and CO₂ (F_{CO_2} , or NEE), according to:

$$\text{ERU} = \frac{F_{\text{COS}}}{[\text{COS}]} \bigg/ \frac{F_{\text{CO}_2}}{[\text{CO}_2]}; \quad \text{ERU} = \frac{F_{\text{COS}}}{\text{NEE}} \times \frac{[\text{CO}_2]}{[\text{COS}]} \quad (3)$$

Broader in scale, an atmospheric relative uptake (ARU; estimated to be ~6; ref. 4) at the local to continental scales can be used to examine the influence of vegetative uptake (and other processes) on the amplitude of the seasonal variations of atmospheric COS and CO₂ (or on vertical gradients observed over terrestrial ecosystems^{3,4}):

$$\text{ARU} = \frac{([\text{COS}]_{\text{spring_max}} - [\text{COS}]_{\text{fall_min}})}{([\text{CO}_2]_{\text{spring_mas}} - [\text{CO}_2]_{\text{fall_min}})} \times \frac{[\text{CO}_2]_{\text{annual_mean}}}{[\text{COS}]_{\text{annual_mean}}} \quad (4)$$

It is generally recognized that the amplitudes of seasonal CO₂ mixing ratio variations throughout the Northern Hemisphere are determined largely by seasonal changes in terrestrial NEE (ref. 15) and inserting equation (2) into equations (3) and (4) provides a potential window to assess GPP/NEE at scales that are not possible at present by other means.

Here we directly explore the links between COS and ecosystem GPP by attempting the first ecosystem-scale eddy covariance flux measurements of COS (F_{COS}), and compare them to estimates based on simultaneous measurements of net CO₂ flux (NEE). We carried out five field campaigns in three pine forests along a steep precipitation gradient (280–710 mm annual precipitation), and in summer and winter crop fields (cotton and wheat, respectively).

¹Environmental Sciences and Energy Research, Weizmann Institute of Science, Rehovot 76100, Israel, ²NOAA-ESRL, Boulder, Colorado 80305, USA.

*e-mail: dan.yakir@weizmann.ac.il.

We used a specially designed mobile laboratory that included an eddy covariance system centred on a fast (20 Hz) CO₂/H₂O infrared gas analyser (IRGA) and a three-dimensional sonic anemometer mounted on a pneumatic mast (4–28 m). The system was complemented by a quantum cascade laser (QCL) system capable of measuring COS and CO₂ at 1 Hz (ref. 10) housed in the temperature-controlled mobile laboratory with air sampling from an intake adjacent to the anemometer.

Background mixing ratios (\pm s.d.) of CO₂ and COS were on average $391 \pm 1.5 \mu\text{mol mol}^{-1}$ and $500 \pm 11 \text{ pmol mol}^{-1}$ respectively, with little diurnal variations during the campaigns (Fig. 1 for a typical day). These levels are consistent with the background records for this latitude (ref. 4, see also <http://www.esrl.noaa.gov/gmd/>), and the local station in the global observation records (<http://www.weizmann.ac.il/GGI/>). The small diurnal variations presumably indicated that rigorous atmospheric mixing overwhelmed the influence of any local vegetation or other processes on mixing ratios.

Canopy eddy covariance flux measurements showed that all sites were sinks for both CO₂ and COS with typical daily cycles peaking around midday (Fig. 1). As indicated above, NEE measurements were based simultaneously on the two analysers, and the comparison between them (Fig. 1) indicated <10% loss of flux in the slow rate measurements. This provided confidence in the COS flux measurements that were obtainable only with the 1 Hz QCL measurements. We also note that although each campaign lasted over a week, the challenges associated with setting up the new and demanding COS measurements at each site reduced the number of successful campaign days.

Midday NEE ranged between -3.9 and $-20.4 \mu\text{mol m}^{-2} \text{ s}^{-1}$ and peak F_{COS} ranged between -50 and $-90 \text{ pmol m}^{-2} \text{ s}^{-1}$, in the dry forest and the cotton field (during the leaf expansion stage). Within this range, the daily sum and daily mean values were obtained and reported in Table 1. As expected, night-time NEE showed small positive fluxes reflecting ecosystem respiration ($2.6 \pm 1.4 \mu\text{mol m}^{-2} \text{ s}^{-1}$, on average across sites). The night-time F_{COS} signal was characterized by a relatively low signal/noise ratio, averaging (\pm s.d.) across sites at $+3.9 \pm 8.6 \text{ pmol m}^{-2} \text{ s}^{-1}$,

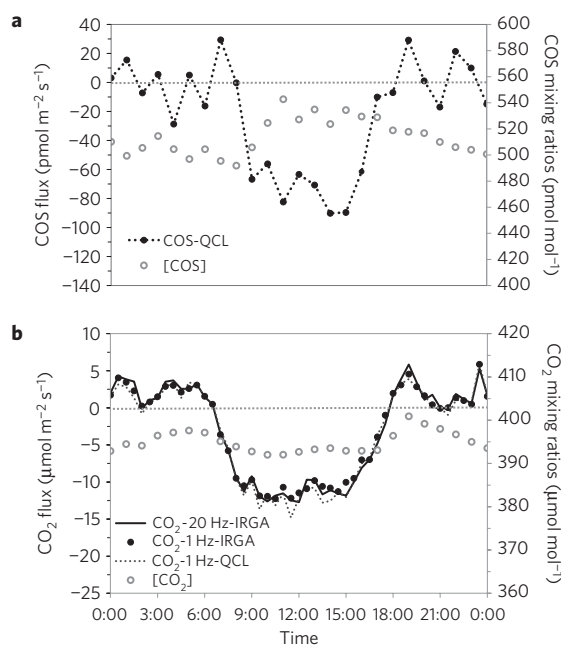


Figure 1 | Daily changes in mixing ratios and fluxes of CO₂ and COS. **a,b**, Typical diurnal cycles in the atmosphere-vegetation COS flux (F_{COS}) above a cotton field, and in the atmospheric COS mixing ratios (pmol mol^{-1}) ~ 3 m above the vegetation canopy (**a**), and in the atmospheric CO₂ mixing ratios ($\mu\text{mol mol}^{-1}$) and net ecosystem CO₂ exchange (NEE; $\mu\text{mol m}^{-2} \text{ s}^{-1}$) measured both with the 20 Hz IRGA and the 1 Hz QCL, with the latter used also for F_{COS} (**b**). Flux loss due to the slow measurements was <10% and often near zero.

emission rates that corresponded to $\sim 6\%$ of the mean midday uptake rates (see example in Fig. 1). To further constrain the soil contribution to F_{COS} , several soil cores (~ 15 cm deep) were collected near the medium-precipitation forest site and on

Table 1 | Exchange fluxes of CO₂ and COS in five field campaigns.

	NEE ($\text{mmol m}^{-2} \text{ d}^{-1}$)	F_{COS} ($\mu\text{mol m}^{-2} \text{ d}^{-1}$)	ERU Daytime	GPP	
				GPP _{COS}	GPP _{Re}
Daytime sum					
	($\text{mmol m}^{-2} \text{ d}^{-1}$)	($\mu\text{mol m}^{-2} \text{ d}^{-1}$)		($\text{mmol m}^{-2} \text{ d}^{-1}$)	($\text{mmol m}^{-2} \text{ d}^{-1}$)
Cotton	-538 ± 29	$-1,764 \pm 65$	2.5	$1,024 \pm 51$	889 ± 46
Wheat	-678 ± 89	$-1,098 \pm 100$	1.3	636 ± 26	680 ± 27
Pine-280	-74 ± 30	-573 ± 239	6.0	329 ± 19	126 ± 6
Pine-520	-424 ± 28	$-1,161 \pm 142$	2.4	458 ± 23	479 ± 20
Pine-710	-414 ± 21.5	$-1,060 \pm 150$	2.0	618 ± 22	503 ± 17
Average	-425 ± 223	$-1,131 \pm 423$	2.8 ± 1.8	612 ± 261	535 ± 281
Daytime mean					
	($\mu\text{mol m}^{-2} \text{ s}^{-1}$)	($\text{pmol m}^{-2} \text{ s}^{-1}$)		($\mu\text{mol m}^{-2} \text{ s}^{-1}$)	($\mu\text{mol m}^{-2} \text{ s}^{-1}$)
Cotton	-13.7 ± 7.6	-43.2 ± 25.5	2.4 ± 0.3	20.6 ± 12.4	17.1 ± 11.8
Wheat	-18.5 ± 13.3	-31.0 ± 22.5	1.3 ± 0.8	16.1 ± 7.5	17.2 ± 7.2
Pine-280	-2.9 ± 1.4	-22.9 ± 23.5	6.1 ± 2.3	8.3 ± 5.2	3.2 ± 1.4
Pine-520	-10.5 ± 6.7	-33.8 ± 33.1	2.5 ± 0.7	10.6 ± 6.3	11.9 ± 5.5
Pine-710	-10.2 ± 4.8	-27.8 ± 38.6	2.1 ± 0.9	15.3 ± 13.9	13.3 ± 5.8
Average	-11.2 ± 5.7	-31.8 ± 7.6	2.9 ± 1.8	14.1 ± 4.8	12.5 ± 5.7

Fluxes were measured by the eddy covariance technique in winter (wheat) and summer (cotton) crops and three pine forests along a precipitation gradient (mean annual precipitation indicated). Net ecosystem exchange of CO₂ (NEE) and COS (F_{COS}) are reported as average daytime sum, and mean values for 9:00–17:00. Number of days averaged for each site varied ($n = 2-6$; see Supplementary Information). Ecosystem relative uptake is the ratio of $F_{\text{COS}}/\text{NEE}$ normalized by the respective ambient mixing ratios ($\sim 390 \mu\text{mol mol}^{-1}$ for CO₂ and $500 \text{ pmol mol}^{-1}$ for COS). GPP_{COS} was obtained from F_{COS} and the ambient mixing ratios using equation (2). GPP_{Re} was obtained using night-time NEE (ref. 19). Daytime sum values represent means for the successful campaign days with s.d. values indicated.

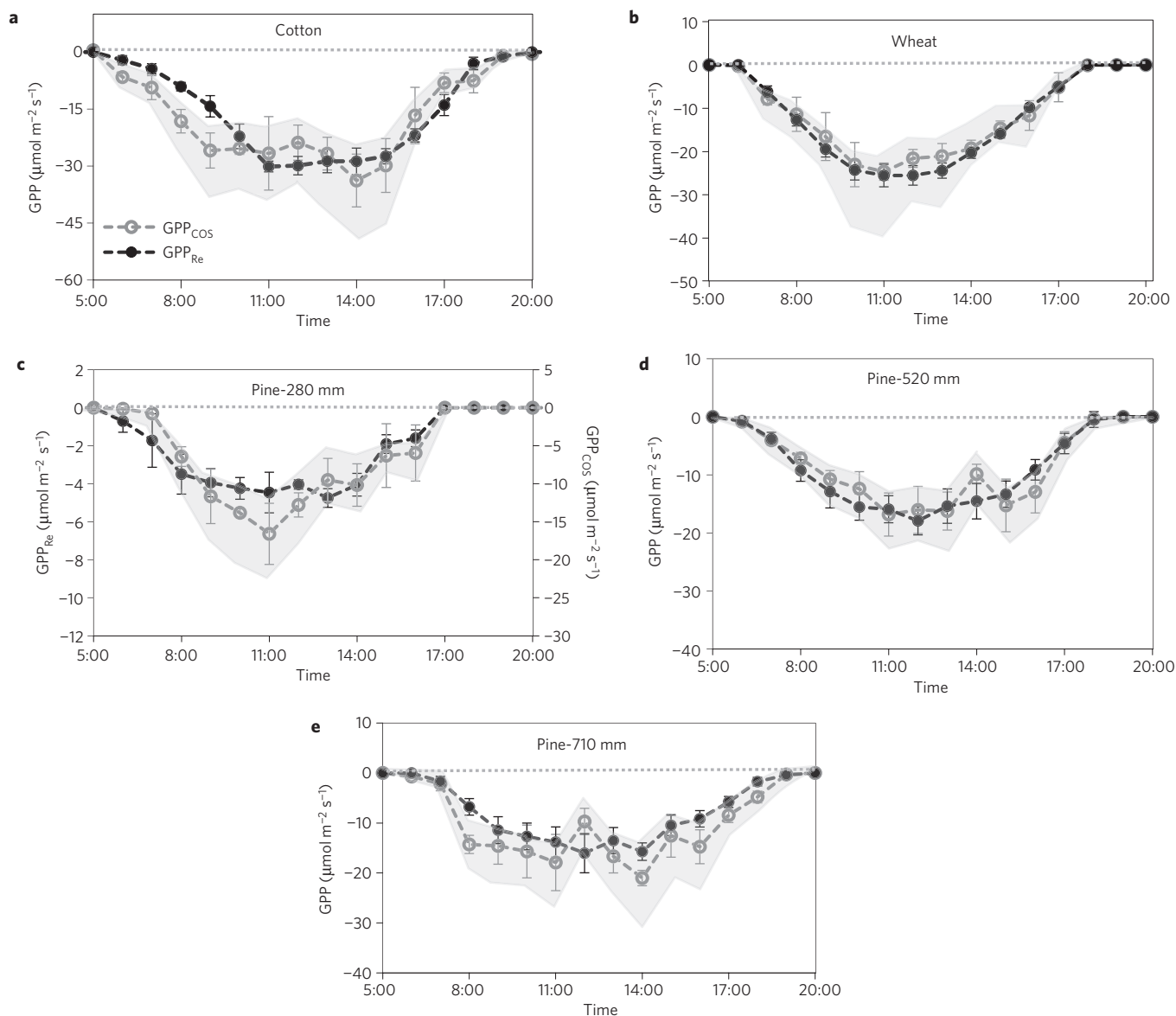


Figure 2 | Diurnal cycles in photosynthetic GPP. **a–e**, Average diurnal cycles in GPP in summer cotton and winter wheat fields (**a,b**), and in three pine forests along a precipitation gradient (**c–e**; mean annual precipitation is indicated). GPP was estimated directly from eddy covariance measurements of F_{COS} (GPP_{COS} , grey circles), or indirectly on the basis of night-time NEE measurements extrapolated to daytime to account for ecosystem respiration (GPP_{Re} , black circles). Shading indicates uncertainty in the GPP estimate associated with variations in LRU between 1 and 2. The number of measurement days represented by each data point varied (see Supplementary Information).

the Weizmann campus, and sealed in specially constructed gas exchange chambers for gas exchange measurements. The results indicated a mean uptake rate across cores and measurement conditions of $-6.6 \text{ pmol COS m}^{-2} \text{ s}^{-1}$, which is within the range of -0.2 to $-13.3 \text{ pmol m}^{-2} \text{ s}^{-1}$ previously reported^{16–19}. The combined records of soil cores and field data (mean values of -6.6 and $+3.9 \text{ pmol COS m}^{-2} \text{ s}^{-1}$) indicate soil fluxes much smaller than daytime uptake, and possibly near zero. A possible explanation is competitive inhibition of the COS uptake by the relevant enzymes due to high soil CO_2 , and the slow rate of non-enzymatic COS hydration²⁰. Further work with increased precision is clearly required to more accurately quantify the soil component.

Using equation (2) and the proposed mean LRU of 1.6 (ref. 6; $\text{LRU}^* \sim 1.5$), we estimated GPP (GPP_{COS}) on an hourly basis at all sites (Fig. 2; night-time GPP = 0 by definition not shown) and report them as daytime mean values, and daily sums (Table 1). The results were compared with GPP_{Re} estimated by a widely used

indirect approach based on night-time NEE representing ecosystem respiration (Re), which is, in turn, extrapolated to daytime values by applying temperature corrections. GPP_{Re} is then obtained from daytime NEE and estimated Re as $\text{GPP} = \text{NEE} + \text{Re}$ (ref. 21). Both approaches have limitations at present, and neither one can serve as an accurate reference⁵. However, GPP_{COS} measurements offer an independent, direct approach, not based on an extrapolated estimate for daytime respiration. Nevertheless, we estimate magnitudes for GPP on the basis of COS fluxes (GPP_{COS}) at all sites and along the climate gradient, which are comparable to those from the more traditional methodology (GPP_{Re}). In all cases GPP estimates from both methods show similar daily cycles and climatic effects (Fig. 2), and values that agree to within $\pm 15\%$ on average (better than $\pm 10\%$ excluding the dry pine forest). Note that the GPP_{COS} values were not adjusted for possible soil contributions. Although this is not necessarily universally applicable, we justify this here given the near-zero night-time fluxes and our soil chamber measurements

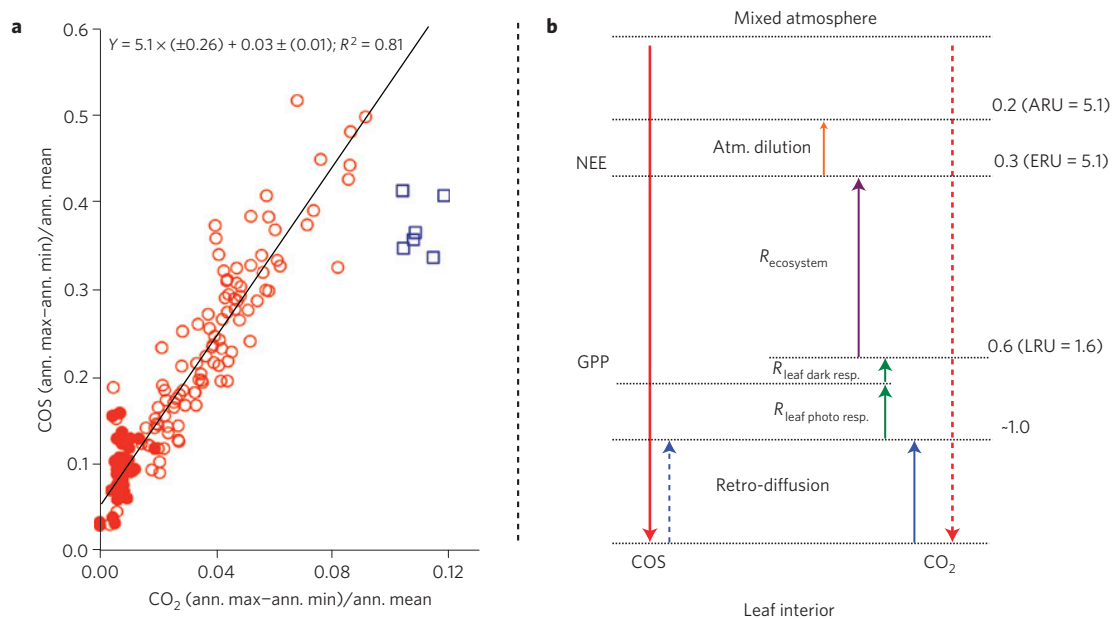


Figure 3 | Relative uptake of COS versus CO₂. **a**, ARU (equation (4)) is the slope (model II linear regression) of seasonal peak-to-peak drawdown of COS versus CO₂ across 15 global sampling stations with up to 12 years of data. Each point represents one year and station; $n = 147$. Stations in the Northern and Southern hemispheres are indicated by empty and filled circles, respectively. Distinct data from Wisconsin USA (squares) and three outliers (outside scale) were excluded from the regression. **b**, The increasing COS/CO₂ flux ratio as respiratory processes diminish net CO₂, but not COS, fluxes with increasing scale (see Supplementary Information for theory), which shows the evolution of the observed ARU slope of 5.1 in **a**.

noted above. We realize that on average, GPP_{COS} values were slightly higher than GPP_{Re} (by $\sim 6\%$ without considering the unusual dry forest site; Table 1), which may result from some soil COS uptake.

An uncertainty in the application of the COS/CO₂ approach presented here is introduced by the use of a constant LRU value^{6–9,22,23}. LRU is related to leaf Ci/Ca (ratio of leaf internal to ambient CO₂ concentrations; see the discussion in the Supplementary Information), which is a relatively conservative parameter in non-stressed plants. It is, however, significantly different in C3 and C4 plants with, consequently C4 LRU of about 1 (ref. 7). Within the same vegetation type, a potential contributor to variations in LRU is variations in the leaf internal conductance (g_m) to COS and CO₂ (refs 9,22). It is generally assumed that stomatal conductance (g_s) dominates the diffusion of both COS and CO₂ into leaves, with g_s/g_m of ~ 0.2 (refs 6,22). However, for example, under environmental stress, internal conductance, g_m , may decrease, and more so for CO₂ with its longer path to the site of carboxylation in the chloroplast, compared with COS hydrolysed closer to the gas/air interface. In this case, higher g_s/g_m and consequently higher LRU values may be expected. This perspective is important because it indicates that LRU may vary mostly upwards compared with the mean value reported^{7,9,22,23}. The sensitivity of inferred GPP_{COS} to the value taken for LRU exhibits a power-law type behaviour (Supplementary Fig. S3), indicating that GPP_{COS} has a low sensitivity to variations in LRU values above the observed mean value of 1.6. In addition, the robustness of the estimated LRU = 1.6 across a wide range of plant species and functional groups⁷, and the good agreement of GPP_{COS} versus GPP_{Re} reported here, based on it, may indicate that in reality, the uncertainty around LRU may have a relatively small influence on estimates of GPP in non stressed plants.

Although ERU is not necessary for estimating GPP, it is an important link of ecosystem- and atmospheric-scale measurements, and allows comparison to reported ARU (equation (4)) values (for example, ref. 4). Estimated ERU based either on the daily sums of F_{COS} and NEE or the daytime mean values (about 9:00–17:00) for each site indicated a mean ERU of about 2.9 ± 1.7 for both cases (Table 1). This value is consistent with the expected values

reported on the basis of less direct approaches of 2.8–4.3 (refs 3,5,9). A higher ERU value of ~ 6 was observed in our dry forest site. This site, however, is characterized by a relatively extensive biological soil crust²⁴, which could enhance the soil uptake of COS and consequently ERU (consistent with $GPP_{COS} \gg GPP_{Re}$ at this site). This suggests the need for a more detailed examination of biological soil crust effects (see ref. 25). Combining equations (2) and (3) yields $ERU/LRU = GPP/NEE$, and using the mean daytime ERU value of 2.9 and LRU* of 1.5 suggests a mean daytime GPP/NEE of ~ 2 . Including night-time NEE in calculating ERU increases the mean, diurnally based ERU to 4.1 and implies a mean GPP/NEE value for our sites of ~ 2.7 , consistent with accepted values²⁶. Note, however, that although these comparisons provide confidence in the new approach, we do expect ERU to vary, and F_{COS}/F_{CO_2} measurements such as proposed here could provide a major tool to identify and quantify this dynamics over space and time.

Finally, as noted above, high-precision measurements of atmospheric COS are performed routinely at now 15 sampling sites around the world, with measurement records being as long as 12 years at some sites (a continuation of work in ref. 4). Combining this record with the CO₂ measurements (<http://www.esrl.noaa.gov/gmd/>) at these same sites, we obtained a robust estimate of ARU (equation (4) and Fig. 3a) of 5.1 ± 0.2 , which is lower than the first estimate made with fewer data⁴ but consistent with the ecosystem values, of 4.1, observed in this study (and with vertical gradients above ecosystems^{3,4}). This atmospheric perspective seems to demonstrate the dominant influence of the land biosphere on the seasonal COS/CO₂ relationships, with LRU of 1.6 increasing to ERU of 4.1, levelling off with ARU of 5.1 (see Fig. 3b for a schematic of this evolution). This may be further supported by ARU values excluded from the global regression line (indicated in Fig. 3a) from Wisconsin that probably reflect the influence of intensive agricultural activities, and the large contribution of C4 vegetation, as data from this site exhibit an ARU of 3.5 ± 0.2 , approximating ecosystem-scale ERU values (Table 1). Considered together, the concentration and flux measurements of COS presented here show that the evolution of the COS/CO₂ relative uptake can be accurately

traced from the leaf, through the ecosystem to the continental scale (Fig. 3b). This is significant because the GPP_{Re} approach can be applied only at the ecosystem scale; at the global atmospheric scale, COS could provide the only means to assess net photosynthesis or GPP in the land biosphere.

Methods

Five field campaigns of 7–14 days each were carried out during 2011–2012 (one during summer 2011, the rest during the winter/spring local active period). Three of the campaigns were carried out in pine forests (predominantly *Pinus halepensis*) along the precipitation gradient in Israel (see Supplementary Information for conditions during the campaigns): dry site (31° 20' 49.2" N 35° 03' 07.2" E; precipitation 280 mm), which is a permanent flux site²⁷ and allowed an inter-comparison of flux measurements between the permanent and mobile flux systems; intermediate site (31° 47' 34.5" N 35° 00' 11.5" E; precipitation 520 mm); wet site in northern Israel (33° 00' 00.5" N 35° 30' 40.5" E; precipitation 710 mm). Two campaigns in crop fields: Cotton field during summer and peak leaf expansion (31° 50' 51.5" N 34° 46' 34.2" E; irrigation 550 mm); wheat field during winter (31° 53' 07.1" N 34° 53' 09.2" E; irrigation 540 mm). A newly designed mobile flux measurement system was used in all campaigns, based on the 30 m pneumatic mast of a 12-ton 4 × 4 truck and a complete eddy flux system. The laboratory provided an air-conditioned instrument facility (cellular communication, 18 KVA generator, 4200 W UPS). Flux, meteorological and radiation measurements rely on an eddy-covariance system that provides CO₂, sensible and latent heat fluxes using a three-dimensional sonic anemometer (R3, Gill Instruments) and closed-path CO₂/H₂O IRGA (Li-Cor 7200) using CarboEuroflux methodology, and EddyPro Software (www.licor.com/). Air temperature and relative humidity (HMP45C probes, Campbell Scientific) and air pressure (Campbell Scientific sensors) were measured ~3 m above the canopy. Energy fluxes rely on radiation sensors including solar radiation (0.29–4.0 μm; CMP21, Kipp and Zonen), long-wave radiation (4.0–100 μm; CRG4, Kipp and Zonen) and photosynthetic radiation (PAR, 0.4–0.7 μm; PAR-LITE2) sensors. All sensors are installed in pairs facing up and down, and they are connected using differential mode through a multiplexer to a data logger (Campbell Scientific). A mid-infrared dual-QCL spectrometer (Aerodyne Research) was used to measure COS and CO₂ concentrations at a frequency of 2,056 cm⁻¹ with a thermoelectrically cooled detector as described previously¹⁰, at a rate of 1 Hz. The inlet tube of the measurements was installed next to a sonic anemometer. A calibration gas mixture for COS was obtained from the National Oceanic and Atmospheric Administration Global Monitoring Division⁴ (NOAA-GMD); CO₂ was calibrated against laboratory tanks that undergo periodic inter-comparison with the NOAA-GMD laboratory. We computed 30-min and 60-min mean fluxes using Eddy-pro 3.0 software. The ratio of the 20 Hz fluxes of CO₂ from the Li-Cor to the 1 Hz measurements of the Li-Cor and the QCL for each 30-min interval provided an estimate of flux loss by instrumental smoothing of high-frequency fluctuations²⁸ (Fig. 1). GPP for each site was estimated using equation (2), and using the conventional approach of estimating ecosystem Re. The latter was carried out using a regression of NEE on turbulent nights against temperature, followed by extrapolating the derived night-time Re–temperature relationship to daytime periods and the relationship: $GPP = NEE + Re$ (ref. 21). Atmospheric mixing ratios for both COS and CO₂ were obtained by the NOAA-GMD global observations network (www.esrl.noaa.gov/gmd/) as described in detail in ref. 4.

Received 4 December 2012; accepted 15 January 2013;
published online 17 February 2013

References

- Raupach, M. R. Pinning down the land carbon sink. *Nature Clim. Change* **1**, 148–149 (2011).
- Pan, Y. *et al.* A large and persistent carbon sink in the World's forests. *Science* **333**, 988–993 (2011).
- Campbell, J. E. *et al.* Photosynthetic control of atmospheric carbonyl sulfide during the growing season. *Science* **322**, 1085–1088 (2008).
- Montzka, S. A. *et al.* On the global distribution, seasonality, and budget of atmospheric carbonyl sulfide (COS) and some similarities to CO₂. *J. Geophys. Res.* **112**, 9302–9317 (2007).
- Blonquist, J. M. *et al.* The potential of carbonyl sulfide as a proxy for gross primary production at flux tower sites. *J. Geophys. Res.* **116**, 4019–4037 (2011).
- Stimler, K., Montzka, S., Berry, J. A., Rudich, Y. & Yakir, D. Relationships between carbonyl sulfide (COS) and CO₂ during leaf gas exchange. *New Phytol.* **186**, 869–978 (2010).
- Stimler, K., Berry, J. A. & Yakir, D. Variations in leaf COS/CO₂ uptake across species and a possible COS mediated H₂S effect on stomatal conductance. *Plant Physiol.* **158**, 524–530 (2011).
- Sandoval-Soto, L. *et al.* Global uptake of carbonyl sulfide (COS) by terrestrial vegetation: Estimates corrected by deposition velocities normalized to the uptake of carbon dioxide (CO₂). *Biogeosciences* **2**, 125–132 (2005).

- Seibt, U., Kesselmeier, J., Sandoval-Soto, L., Kuhn, U. & Berry, J. A. A kinetic analysis of leaf uptake of COS and its relation to transpiration, photosynthesis and carbon isotope fractionation. *Biogeosciences* **7**, 333–341 (2010).
- Stimler, K., Nelson, D. & Yakir, D. High precision measurements of atmospheric concentrations and plant exchange rates of carbonyl sulfide (COS) using mid-IR quantum cascade laser. *Glob. Change Biol.* **16**, 2496–2503 (2010).
- Bruhl, C., Lelieveld, J., Crutzen, P. J. & Tost, H. The role of carbonyl sulphide as a source of stratospheric aerosol and its impact on climate. *Atmos. Chem. Phys.* **12**, 1239–1253 (2012).
- Watts, S. F. The mass budgets of carbonyl sulfide, dimethyl sulfide, carbon disulfide and hydrogen sulfide. *Atmos. Environ.* **34**, 761–779 (2000).
- Kettle, A. J. *et al.* Comparing forward and inverse models to estimate the seasonal variation of hemisphere-integrated fluxes of carbonyl sulfide. *Atmos. Chem. Phys.* **2**, 343–361 (2002).
- Protoschill-Krebs, G. & Kesselmeier, J. Enzymatic pathways for the metabolism of carbonyl sulphide (COS) by higher plants. *Bot. Acta* **108**, 445–448 (1992).
- Baldocchi, D. *et al.* FLUXNET: A new tool to study the temporal and spatial variability of ecosystem-scale carbon dioxide, water vapor, and energy flux densities. *Bull. Am. Meteorol. Soc.* **82**, 2415–2434 (2001).
- Kesselmeier, J., Teusch, N. & Kuhn, U. Controlling variables for the uptake of atmospheric carbonyl sulfide (COS) by soil. *J. Geophys. Res.* **104**, 11577–11584 (1999).
- Steinbacher, M., Bingemer, H. G. & Schmidt, U. Measurements of the exchange of carbonyl sulfide (OCS) and carbon disulfide (CS₂) between soil and atmosphere in a spruce forest in central Germany. *Atmos. Environ.* **38**, 6043–6052 (2004).
- Kuhn, U. *et al.* Carbonyl sulfide exchange on an ecosystem scale: Soil represents a dominant sink for atmospheric COS. *Atmos. Environ.* **33**, 995–1008 (1999).
- Yi, Z. *et al.* Soil uptake of carbonyl sulfide in subtropical forests with different successional stages in south China. *J. Geophys. Res.* **112**, 8302–8313 (2007).
- Sandoval-Soto, L., Kesselmeier, M., Schmitt, V., Wild, A. & Kesselmeier, J. Observations of the uptake of carbonyl sulfide (COS) by trees under elevated atmospheric carbon dioxide concentrations. *Biogeosciences* **9**, 2935–2945 (2012).
- Reichstein, M. *et al.* On the separation of net ecosystem exchange into assimilation and ecosystem respiration: Review and improved algorithm. *Glob. Change Biol.* **11**, 1424–1439 (2005).
- Seibt, U., Rajabi, A., Griffiths, H. & Berry, J. A. Carbon isotopes and water use efficiency: Sense and sensitivity. *Oecologia* **155**, 441–454 (2008).
- Wohlfahrt, G. *et al.* Carbonyl sulfide (COS) as a tracer for canopy photosynthesis, transpiration and stomatal conductance: Potential and limitations. *Plant Cell Environ.* **35**, 657–667 (2012).
- Wilske, B. *et al.* The CO₂ exchange of biological soil crusts in a semiarid grass-shrubland at the northern transition zone of the Negev desert, Israel. *Biogeosciences* **5**, 1411–1423 (2008).
- Kuhn, U. & Kesselmeier, J. Environmental variables controlling the uptake of carbonyl sulfide by lichens. *J. Geophys. Res.* **105**, 26783–26792 (2000).
- Falge, E. *et al.* Seasonality of ecosystem respiration and gross primary production as derived from FLUXNET measurements. *Agri. Forest Meteorol.* **113**, 53–74 (2002).
- Grunzweig, G. M., Lin, T., Rotenberg, E., Schwartz, A. & Yakir, D. Carbon sequestration in arid-land forest. *Glob. Change Biol.* **9**, 791–799 (2003).
- Goulden, M. L., Munger, J. W., Fan, S. M., Daube, B. C. & Wofsy, S. C. Measurements of carbon sequestration by long-term eddy covariance: Methods and a critical evaluation of accuracy. *Glob. Change Biol.* **2**, 169–182 (1996).

Acknowledgements

We are grateful to G. Fratini for help using EddyPro, and to M. Cuntz, G. Wohlfahrt and J. Berry for helpful discussions. The technical help of H. Sagi and A. Pelter are gratefully acknowledged. This work was made possible by financial support from the Israel Science Foundation (ISF), the Minerva foundation, the JNF-KKL, and the C. Wills and R. Lewis program in Environmental Science.

Author contributions

D.Y. conceived the study. D.A. performed all COS measurements. D.A., E.R., U.D. and F.T. carried out all of the field measurements and data analysis. S.A.M. provided the atmospheric data. D.Y. and D.A. wrote the paper with discussions and contributions to interpretations of the results from all co-authors.

Additional information

Supplementary information is available in the online version of the paper. Reprints and permissions information is available online at www.nature.com/reprints. Correspondence and requests for materials should be addressed to D.Y.

Competing financial interests

The authors declare no competing financial interests.